AIAA JOURNAL
Vol. 46, No. 5, May 2008

Technical Notes

TECHNICAL NOTES are short manuscripts describing new developments or important results of a preliminary nature. These Notes should not exceed 2500 words (where a figure or table counts as 200 words). Following informal review by the Editors, they may be published within a few months of the date of receipt. Style requirements are the same as for regular contributions (see inside back cover).

Buckling Modes of Thin Circular Cylindrical Shells Under Fundamental Loads

Yoichi Hirano*
Chuo University, Tokyo 112-8551, Japan

DOI: 10.2514/1.36072

Introduction

OVER the past 100 years, much research has been directed at circular cylindrical shell buckling. One area of particular interest is in clarifying the reasons for the discrepancy between theoretical and experimental buckling stress of thin isotropic circular cylindrical shells, especially under axial compression. Postbuckling behavior, initial imperfections, or boundary conditions have been used to explain the discrepancy, although the main causes are now considered to be the effects of initial imperfections and their relationship to postbuckling characteristics [1,2]. The effects of boundary conditions, on the other hand, were discussed by Hoff [3], who showed that axial buckling stress calculated for the special boundary conditions is one-half of the classical value. The employed boundary conditions, however, are considered to be unrealistic [4]. Yoshimura [5] attributed postbuckling characteristics under axial compression to the developability of the initial cylindrical surface; that is, the Gauss curvature equals zero. The postbuckling mode presented by Yoshimura is a developable polyhedral surface (Fig. 1a) that is different from the chessboard-type (rectangle-type) mode and was named the "Yoshimura pattern" by Hoff et al. [6]. Key references related to the present problem are found in texts by Yamaki [7] and Singer et al. [8]. In recent years, numerous studies have focused on buckling of composite or laminated cylindrical shells. For example, Riddick and Hyer [9] employed finite element analysis for segmented circular composite cylindrical models under axial compression, ultimately showing calculated postbuckling modes.

Here, it is shown that the developability of cylindrical surfaces also leads to buckling mode patterns under torsional load (Fig. 2a) and external lateral pressure (Fig. 2b). Such developability leads to buckling and postbuckling characteristics that are quite different from flat-plate problems. In other words, the developability provides the mechanics of the cylindrical shell buckling process. It is concluded that

1) Buckling and postbuckling modes under axial compression should be the same.

2) The number of waves may change during the postbuckling process.

Received 6 December 2007; revision received 23 January 2008; accepted for publication 25 January 2008.

*Professor, Faculty of Science and Engineering. Senior Member AIAA.

Moreover, the axial buckling modes should be similar to the modes described by Yoshimura [5], being different from the so-called chessboard pattern that has been traditionally been used in previous studies.

Buckling Modes

Differential geometry is used to show that a cylindrical surface is developable due to the Gauss curvature being equal to zero, which allows us to tessellate various types of polygons on deployed flat surfaces. When flat surfaces tessellated by triangles (Fig. 3a) are wrapped cylindrically the circular cylindrical surfaces can be deformed into the Yoshimura pattern (Fig. 1a), which has sharp inward and outward ridges and flat triangular surfaces, being quite different from the original cylindrical surface. The bold and thin lines in Fig. 3a correspond, respectively, to outward and inward ridges (fold lines), whereas the triangular surface is inextensional. If the ratio of thickness to radius is very small, the ridges contain most strain energy during buckling. For plate buckling, both extensional and bending strain energy play the role during buckling; that is, the flat plates do not have a developable surface other than the original flat surface. Flat surfaces tessellated with more general polygons (Fig. 3b) can also be wrapped cylindrically, having outward and inward ridges (Fig. 1b). A pattern similar to that shown in Fig. 3b was observed by Coppa [10] during impact buckling experiments, whereas the patterns shown in Figs. 2a and 2b look like the buckling modes calculated by Yamaki [7] under torsion and under external lateral pressure. These modes can be deployed on flat surfaces if the boundary conditions at both edges of the cylinder are not considered (Figs. 4a and 4b). Such patterns and the Yoshimura pattern are special cases of Fig. 1b. The flat surfaces tessellated with the so-called chessboard or rectangular pattern (Fig. 5) can also be wrapped into circular cylinders surfaces, but do not exhibit sharp inward and outward fold lines or flat rectangles, because horizontal lines are at right angles to the vertical lines. This pattern has been conventionally used to represent the axial buckling mode to solve the problem. However, patterns like Yoshimura's have only been used in analysis to represent the postbuckling mode and not the buckling mode. In contrast, it is confirmed here using an analytical approach that the buckling mode should be the same mode as in the postbuckling region, except for the number of waves.

Axial Buckling Mode

Cheng and Ho [11] showed that for anisotropic circular cylindrical shells, Flugge's buckling differential equations and given boundary conditions can be solved exactly for torsion and external lateral pressure, although they did not try to solve the axial buckling problem, for some unknown reason. The basic differential equations are shown as follows:

$$a^2\frac{\partial^2 u}{\partial x^2}+\frac{1-\nu}{2}\frac{\partial^2 u}{\partial \theta^2}+\frac{1+\nu}{2}a\frac{\partial^2 v}{\partial x\partial\theta}+\nu a\frac{\partial w}{\partial x}+k\left(\frac{1-\nu}{2}\frac{\partial^2 u}{\partial\theta^2}-a^3\frac{\partial^3 w}{\partial x^3}+\frac{1-\nu}{2}a\frac{\partial^3 w}{\partial x\partial\theta^2}\right)-q_2a^2\frac{\partial^2 u}{\partial x^2}=0$$

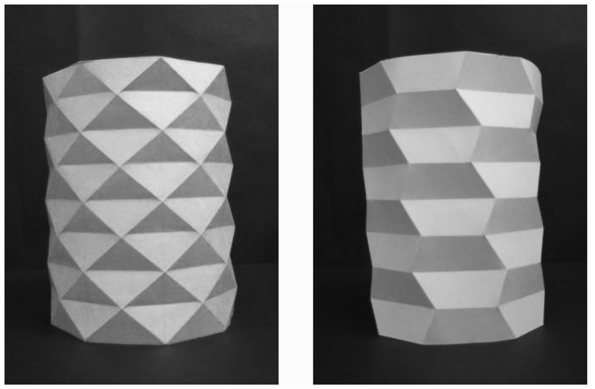

a) b)

Fig. 1 Buckling mode of thin circular cylindrical shells: a) Yoshimura pattern under axial compression and b) general polygon pattern.

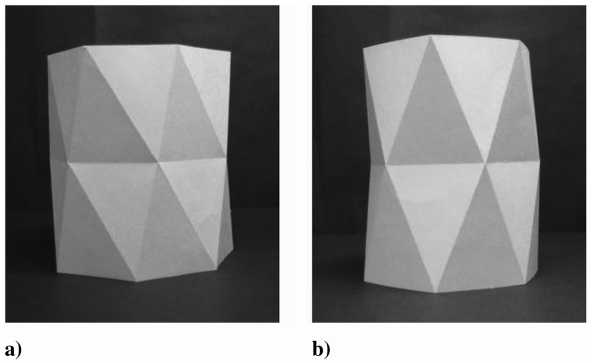

a) b)

Fig. 2 Buckling mode a) under torsion and b) under external lateral pressure.

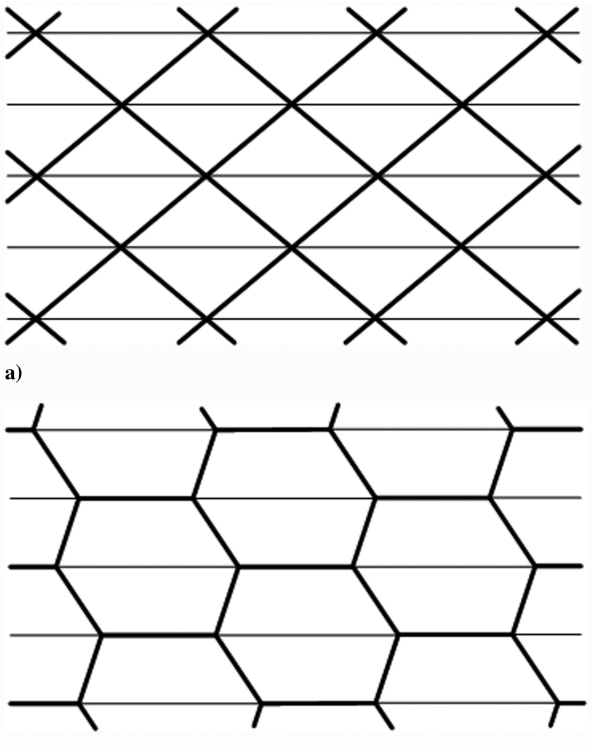

a)

b)

Fig. 3 Flat surface tessellated with the a) Yoshimura pattern and b) general polygon pattern.

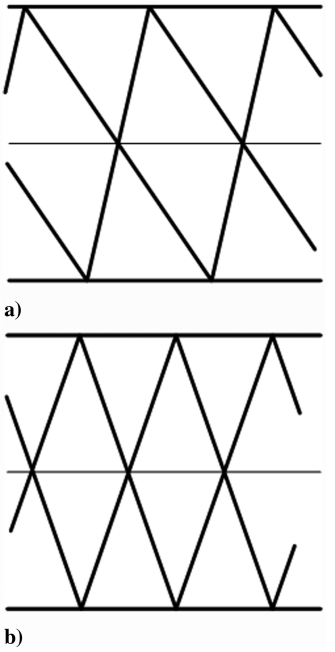

a)

b)

Fig. 4 Developed a) torsional and b) external lateral pressure patterns.

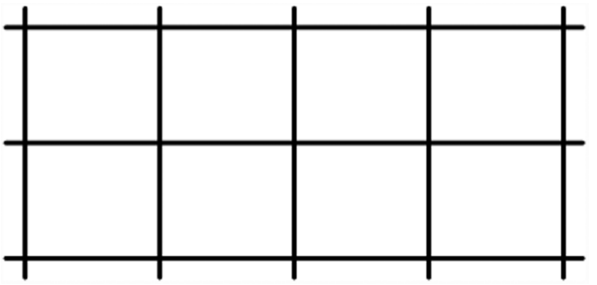

Fig. 5 Rectangle (chessboard) pattern usually assumed for axial buckling mode.

$$\frac{1+\nu}{2}a\frac{\partial^2 u}{\partial x\partial\theta}+\frac{\partial^2 v}{\partial\theta^2}+\frac{1-\nu}{2}a^2\frac{\partial^2 v}{\partial x^2}+\frac{\partial w}{\partial\theta}+k\left\{\frac{3}{2}(1-\nu)a^2\frac{\partial^2 v}{\partial x^2}-\frac{3-\nu}{2}a^2\frac{\partial^3 w}{\partial x^2\partial\theta}\right\}-q_2a^2\frac{\partial^2 v}{\partial x^2}=0$$

$$\nu a\frac{\partial u}{\partial x}+\frac{\partial v}{\partial\theta}+w+k\left(\frac{1-\nu}{2}a\frac{\partial^3 u}{\partial x\partial\theta^2}-a^3\frac{\partial^3 u}{\partial x^3}-\frac{3-\nu}{2}a^2\frac{\partial^3 v}{\partial x^2\partial\theta}+a^4\frac{\partial^4 w}{\partial x^4}+2a^2\frac{\partial^4 w}{\partial x^2\partial\theta^2}+\frac{\partial^4 w}{\partial\theta^4}+2\frac{\partial^2 w}{\partial\theta^2}+w\right)+q_2a^2\frac{\partial^2 w}{\partial x^2}=0 \tag{1}$$

where x and θ are the axial and circumferential coordinates; a is the radius; u, v, and w are the axial, circumferential, and normal buckling displacement, respectively; $k=t^2/(12a^2)$; $q_2=P(1-\nu^2)/(Et)$; and t, P, E, and ν are, respectively, the thickness, applied axial load, Young's modulus, and Poisson's ratio.

The deflection functions u, v, and w are assumed and are likewise used for the buckling mode under torsion; that is,

$$u=U\sin[(\lambda x/a)+n\theta] \qquad v=V\sin[(\lambda x/a)+n\theta]$$
$$w=W\cos[(\lambda x/a)+n\theta] \tag{2}$$

where n is the circumferential wave number, $\lambda=m\pi a/L$, and m and L are the number of axial half-waves and cylinder length.

The deflection functions in Eq. (2) were used for axial buckling of filament wound cylinders by Tasi et al. [12] to satisfy Eq. (1).

Substitution of Eq. (2) into Eq. (1) yields characteristic buckling equations for isotropic materials expressed as Eq. (A6) by Cheng and Ho [11]. When the first estimate of axial buckling load is given, the eight roots of the characteristic equation (eighth-degree polynomial of λ) are calculated for the given dimensions, material properties, and assumed circumferential wave number n; therefore, eight terms are considered for the deflection functions u, v, and w. The deflection functions given by Eq. (2) must also satisfy the boundary conditions

$$u = v = w = \partial w/\partial x = 0$$

at $x = \pm L/2$ for the case in which both edges are clamped. The axial buckling load is changed iteratively to satisfy both the characteristic equations and boundary conditions until convergence. Note that the eight terms of Eq. (2) can satisfy both the buckling differential equations and boundary conditions. Details of the numerical procedure are in a report by Tasi et al. [12]. The axial buckling mode assumed in most previous research has been the chessboard pattern, which cannot express a pattern such as Yoshimura's. However, a Yoshimura-like pattern has been used for the postbuckling region; for example, Yamaki [7] assumed Eq. (2.10.4) to represent the axial buckling mode:

$$\begin{gathered} u = U\exp(i\lambda x/a)\cos n\theta \qquad v = V\exp(i\lambda x/a)\sin n\theta \\ w = W\exp(i\lambda x/a)\cos n\theta \end{gathered} \tag{3}$$

where $i = \sqrt{-1}$. Eight terms with a different λ value in Eq. (3) also satisfy the axial buckling differential equations and boundary conditions. The preceding mode for w is the rectangle pattern shown in Fig. 5 and has the zero of w on lines $\theta =$ constant (generator); therefore, Yamaki [7] only shows the axial distribution of the buckling deflection. Weaver [13] and Wong and Weaver [14] derived analytical expressions for an axial buckling load on composite cylinders, using the same buckling deflection as Eq. (2). However, they use only one term, such that their deflection function cannot satisfy the boundary conditions.

Conclusions

The developability of circular cylindrical shells gives the buckling modes under torsion and external lateral pressure just as for the case under axial compression. The buckling and postbuckling modes should be represented using a pattern similar to that used by Yoshimura, in which the number of waves may change during the postbuckling process.

Acknowledgment

The author would like to thank Akane Kojima for assistance in preparing the manuscript.

References

[1] Donnell, L. H., and Wan, C. C., "Effect of Imperfections on Buckling of Thin Cylinders and Columns under Axial Compression," *Journal of Applied Mechanics*, Vol. 17, Mar. 1950, pp. 73–83.

[2] Koiter, W. T., "On the Stability of Elastic Equilibrium," NASA TT-F-10833, 1967.

[3] Hoff, N. J., "Low Buckling Stresses of Axially Compressed Circular Cylindrical Shells of Finite Length," *Journal of Applied Mechanics*, Vol. 32, Sept. 1965, pp. 203–211.

[4] Teng, J. G., "Buckling of Thin Shells: Recent Advances and Trends," *Applied Mechanics Reviews*, Vol. 49, No. 4, 1996, p. 263.

[5] Yoshimura, Y., "On the Mechanism of Buckling of a Circular Cylindrical Shell Under Axial Compression," NACA TM 1390, 1955.

[6] Hoff, N. J., Madsen, W. A., and Mayers, J., "Postbuckling Equilibrium of Axially Compressed Circular Cylindrical Shells," *AIAA Journal*, Vol. 4, Jan. 1966, pp. 126–132.

[7] Yamaki, N., *Elastic Stability of Circular Cylindrical Shells*, North-Holland, New York, 1984.

[8] Singer, J., Arbocz, J., and Weller, T., *Buckling Experiments: Experimental Methods in Buckling of Thin-Walled Structures*,Vol. 2, Wiley, New York, 2002.

[9] Riddick, J. C., and Hyer, M. W., "Postbuckling Behavior of Segmented Circular Composite Cylinders," *AIAA Journal*, Vol. 42, No. 1, 2004, pp. 185–195. doi:10.2514/1.9042

[10] Coppa, A. P., "The Buckling of Circular Cylindrical Shells Subject to Axial Impact," *Collected Papers on Instability of Shell Structures*, NASA TN D-1510, 1962, pp. 361–400.

[11] Cheng, S., and Ho, B. P. C., "Stability of Heterogeneous Aeolotropic Cylindrical Shells Under Combined Loading," *AIAA Journal*, Vol. 1, No. 4, 1963, pp. 892–898.

[12] Tasi, J., Feldman, A., and Stang, D. A., "The Buckling Strength of Filament-Wound Cylinders Under Axial Compression," NASA CR-266, 1965.

[13] Weaver, P. M., "Anisotropy-Induced Spiral Buckling in Compression-Loaded Cylindrical Shells," *AIAA Journal*, Vol. 40, No. 5, 2002, pp. 1001–1007.

[14] Wong, K. F. W., and Weaver, P. M., "Approximate Solution for the Compression Buckling of Fully Anisotropic Cylindrical Shells," *AIAA Journal*, Vol. 43, No. 12, 2005, pp. 2639–2645. doi:10.2514/1.10924

A. Palazotto
Associate Editor